REVIEW OF THE INTERCEPT METHOD FOR RELATIVE PERMEABILITY CORRECTION USING A VARIETY OF CASE STUDY DATA

Jules Reed[1], Jos Maas[2]
(1) Lloyd's Register, Aberdeen, UK (2) Independent Consultant

This paper was prepared for presentation at the International Symposium of the Society of Core Analysts held in Trondheim, Norway, 27-30 August 2018

ABSTRACT

In 2014, Gupta and Maloney[1] introduced a novel method of measuring steady state relative permeability, called the Intercept Method. The Intercept Method entails a modification of a standard steady state procedure that incorporates multiple total flow rates at each fractional flow rate. The objective of the method is to measure data at each fractional flow rate that will permit simple analytical calculations to correct differential pressure (hence relative permeability) and saturation data for the effects of capillary pressure. The Intercept Method is intended to provide a corrective technique without the need for additional supportive analyses, such as capillary pressure and in situ saturation monitoring (ISSM), or as an alternative approach to the current considered best practice of numerical coreflood simulation, which generally requires the specified additional data.

Consequently, the Intercept Method is of interest to the global industry in regions and/or laboratories that do not possess state-of-the-art equipment, or for its cost saving potential. However, before employing this new method, it was important to the authors to investigate its validity across the range of rock properties, sample dimensions and wettabilities experienced in commercial SCAL coreflood experiments. This study thus draws on a variety of relative permeability curves (and supporting data) from various global core studies, originally derived by typical relative permeability methods plus coreflood simulation. From these data, we use SCORES to simulate the expected results of multi-flowrate steady state experiments and use the Intercept Method to derive and compare the corrected relative permeability curves. Results highlight criteria under which the method does not provide fully corrected data. The paper explores these criteria in more detail.

INTRODUCTION

Core analysis is designed to provide quantitative information of reservoir properties, from limited available material, that can be used to aid interpretation of more widely available but more qualitative measurements such as seismic data and log measurements. The reservoir properties of interest to petroleum scientists, can be split largely into two main categories: static properties, such as capillary pressure, and dynamic properties, like relative permeability. Static properties describe reservoir endpoints achieved through geological timescales, such as connate water saturation driven by hydrocarbon migration, or after substantial human intervention, such as expected final saturations in fully swept layers or

regions; whilst dynamic properties describe the movement of fluids during a changing environment, such as water influx during production because of water injection or because of an active aquifer. In a hydrocarbon reservoir, due to the large length-scales, these properties are mostly independent of one another; however, in laboratory based core analysis these properties exhibit mutual interference due to the small length-scales. Mutual interference means that static and dynamic properties are inextricably linked during laboratory testing, i.e. capillary pressure measurements are impacted by the relative permeability of the fluids and relative permeability measurements are influenced by capillary pressure.

To achieve static capillary pressure conditions in laboratory tests, fluids must first be displaced, e.g. for primary drainage, water must be displaced from the fully water saturated core plug under the influence of pressurised hydrocarbon. Fluid displacement rates change dependent upon relative permeability at specific saturation values: e.g. as water saturation decreases, relative water permeability decreases and hence, effective water permeability decreases, slowing water production rates and extending test time. It is essential in static property analysis, to allow sufficient time to achieve static (or near-static) conditions, else error will be introduced to the results. Thus, static property test times will be impacted by relative permeability and the results will be impacted by the actual length of time employed by labs, compared to what should be required to extend to static conditions.

Relative permeability experiments are impacted by capillary pressure, such that fluid saturations are determined as a function of pore throat (and/or pore) radii, core wettability and the balance of fluid pressures during flow conditions. Hence, the influence of capillary pressure becomes a function of differential pressure (dP) which is decreasing from the inlet face (largest viscous displacement force for the given test conditions) and tending to zero at the outlet (production) face, where capillary forces will dominate. This results in an outlet-face saturation which will always be determined by spontaneous wetting forces and a potentially changing saturation with sample length towards the inlet-face (increasing dP), giving rise to the capillary end effect. During relative permeability analysis, the impact of capillary pressure will vary dependent upon the method, average saturation and flow rates.

Various methods have been considered to attempt to reduce these effects: using scaling criteria to increase the ratio of viscous to capillary forces; increasing flow rates, increasing sample length (Rapoport & Leas[3], Batycky[4]); using pressure taps along the sample attempting to keep the capillary end effect outside so that unaffected data lies within the pressure capture region (e.g. Chen & Wood[5] and van der Post, et al.[6]); using core pieces as endstems attempting to capture the end effect within the core pieces; but capillary end effects may not be sufficiently minimised or fully removed by these methods, particularly where composite cores are used which may exhibit capillary end effects occurring at core intersections.

Simulation methods, that derive relative permeability by accounting for capillary pressure and matching test measurements, can be difficult and require additional data inputs: capillary pressure and preferably in situ saturation monitoring (ISSM). The use of additional input

data requires stringent quality control measures throughout all stages of the core analysis process to ensure that relative permeability and capillary pressure data are performed on correlated, representative samples.

The intercept method provides a potential alternative method to acquire relative permeability, without the additional capillary pressure or ISSM data, using simple analytical calculations to derive relative permeability by correcting for capillary end effects.

DISCUSSION OF PHYSICAL PRINCIPLES OF THE METHOD

To understand the intercept method, we will first review the physics of the capillary end effect. In a flooding experiment, just outside the end face of the core plug, the meniscus between two escaping fluids has little or no curvature, because the fluid collection system in the end flange of the apparatus has channels of a dimension much larger than the pore sizes in the plug. Consequently, the capillary pressure just outside the plug will be close to zero, i.e. the pressures in the two phases will be identical. Because of pressure continuity, the pressures of the two phases near the exit face just inside the plug will then also be close to identical.

Inside the core plug, the capillary pressure plot links the difference in phase pressure to a local saturation. So, near the exit, the local saturation is likely to be almost a constant value given by Pc=0, throughout the experiments. Upstream in the core plug the saturation values likewise are determined by the balance between viscous and capillary forces.

Near the entry face, saturation is driven by the injected fractional water flow (fw), while viscous forces and capillary forces are keeping their balance. The capillary pressure linked to the saturation, “asked for” by the governing fw curve, cannot surpass the viscous pressure drop in the more mobile phase. If it would, a negative pressure gradient would come about in the displaced phase at the entry face. In effect, any flooding experiment, whether steady-state or an unsteady-state (Welge) experiment, is limited in the maximum capillary pressure it can probe due to limitations in the laboratory. High flow rates will interfere at some point with the integrity of the core plug due to the migration of fines or the plug may just break down at a high pressure drop. This is the reason that true residual oil or connate water can never be achieved in a flooding experiment.

Gupta and Maloney[1] suggested that with increasing total flow rate (Qt), at a given constant fractional flow, the saturation distribution in the core plug approximately will maintain a constant average saturation. With the saturation at the entry point being constant because it is governed by a constant fw, the saturation profile in the plug gets compressed in shape, but the total saturation range does not change. Based on that assumption they were able to derive two correction procedures: one to correct the pressure drop for the impact of capillary forces and another one to correct the average saturation (as observed from material balance) for the impact of the capillary forces on the saturation profile. For details, see Refs. 1 and 2.

It is not a priori clear when this approximation of the water saturation being a constant in the end-effect zone may break down. For that reason, we have tested the method on cases with a large variety of wettability, i.e. of curvature of the capillary pressure function.

CASE STUDIES

A review of the intercept method was performed by simulating in SCORES[7], the multi-rate steady state technique using relative permeability and capillary pressure data from a number of case studies, on core plugs of varying dimensions, reservoir properties and wettability and various fluid properties. The samples represented a variety of dimensions often used in commercial laboratory analysis, from below 5 cm and up to 9 cm on single plugs, and a composite core.

Six cases were reviewed: Case0 - the original data from Gupta and Maloney[1]; Case1 - core from UKCS sandstone, mixed wet; Case2- core from South American sandstone, slightly water wet; Case3 –core from UKCS sandstone, mixed to water wet; Case4 –core from UKCS sandstone, Brent formation, slightly oil wet; Case5 – middle east carbonate, slightly water wet. Table 1 provides the core plug and fluid properties input to the simulations. Relative permeability (kr) and capillary pressure (Pc) curves were obtained from model data; Corey and Skjaeveland models, respectively. The Corey and Skjaeveland model parameters for each case also are provided in Table 1, and plotted on a combined graph in Figure 2. For each case (Case1 – Case5) relative permeability had been derived by simulation of experimental data using capillary pressure from a representative plug (from the same rock type with similar properties – see Table 1). The simulation history match data of cases 1 through 5 are provided in Figure 3 through Figure 7. Table 1 also provides the total flow rates used for each case. NB. Bracketed values are those used in the final fraction (fw=1), where deemed necessary, attempting to decrease the impact of capillary end effects.

Case 0

Figure 8 shows the results of repeating the analysis by Gupta & Maloney[1]. Figure 8 (left) shows the resultant relative permeability curve and (right) shows the saturation profiles. The data provided a match to the input relative permeability. Expected Sor was 0.2; IM predicted 0.203 (well within laboratory measurable saturation error). Krw endpoint was expected to be 0.65; IM predicted between 0.637 and 0.647, a maximum 2% error (again, well within measurable laboratory error). However, an impractical time of at least 1000 years (!) was required to achieve stable conditions during fw=1, owing to the extremely low oil relative permeability ($< 10^{-10}$) in the final few saturation units, but achieving stable conditions was discovered to be essential for the intercept method (IM) to successfully derive corrected relative permeability and saturation close to residual conditions.

Case 1

Figure 9 (left) shows the results of Case1 relative permeability curves from UKCS mixed wet sandstone. The lines are the input relative permeability curves. The open circles are the results that would be obtained from the conventional (Darcy) calculations from standard steady state data. The filled diamonds are the results using the intercept method (IM). These

show dependable corrected data through all fractions, except at the final fraction, fw=1. Figure 9 (right) shows saturation profiles, where each Qt is plotted using different line formatting. The plot indicates that the capillary end effect (CEE) has been captured within the sample length for most of the saturation profiles, except at fw=1 (the upper 4 lines). At fw=1, the CEE extends beyond the length of the sample so that regression of dP versus Qt will not produce a correct offset, thus true kr and true Sw cannot be extrapolated. As an improved example of this phenomenon, Figure 14 shows two different plots of saturation profiles; one capturing the entire CEE within the sample (left) and the other (right) not capturing the CEE within the sample length.

Case 2

Case 2 is a slightly water wet plug from a South American sandstone. Relative permeability results are shown in Figure 10, again showing excellent corrected data, though again failing to extrapolate to true residual oil saturation, since the CEE (captured within the sample length for all previous fractional flow rates) is not captured within the sample.

Case3

Case 3 (see Figure 11) was a water to mixed wet high permeability (almost 3D) composite core plug, created from 4 individual samples from a single, homogeneous whole core preserved section. Results were excellent until Sw increased above approximately 0.70, which required high fw rates (0.999). As can be observed in the saturation profiles, the CEE was not captured within the sample length for the final two fractions, despite the sample being 32 cm in length. In addition, the simulations do not account for the potential for multiple internal end effects between the 4 composite stacked core samples. Residual oil saturation is not achieved. Initial attempts to simulate this case, failed due to insufficient time provided for certain fw, particularly at high fw values, to achieve steady state. If steady state had not been sufficiently reached, the IM calculations did not work well for the unstable fractions. Times and flow rates (fw and Qt) were adjusted and optimised to achieve the final simulations presented. However, Qt was limited to 480 cc/h, since many commercial laboratories use pumps with limited flowrates, and very high flow rates may be detrimental to the core material, possibly promoting fines or grain migration, or turbulent flow. Time optimisation for Case 3 implies that 20 days would be required, merely to complete fw=1 at all 4 fractional flow rates (see Figure 15 – right). An earlier simulation of Case3 (Figure 15 – left) shows that fw=1 does not stabilise within a coreflood lasting 23 days in total. Subsequent (and previous) simulations were performed using various parameters to attempt to optimise the steady state conditions.

Case 4

Case4 (Figure 12) was a slightly oil wet sandstone. Early fractional flow rates produce results (filled diamonds) not quite matching the expected relperm curves (lines). IM calculations appear to overestimate kr at these lower saturations, although they are a much-improved correlation over those that would be derived from standard steady state analytics (open circles). The open circles can be observed to fall in 4 distinct curves, each relating to a particular flow rate. As fw increases, the IM krw curve begins to fall below the expected

curve, whilst kro remains higher than expected kro. Residual oil saturation was not achieved.

Case 5

Case5 (Figure 13) is a slightly water wet carbonate from the middle east. IM calculations produced a good correlation to the expected relative permeability curves. However, there is a small mismatch in krw at the higher saturations – IM krw is slightly lower than expected, but within ±5% error expected in measurements for this permeability range. However, final water saturation (Swf) at residual oil saturation was correctly regressed (0.79). It is worth noting that this is the only case (of those studied) where true residual oil saturation was achieved, even after increasing total flow rates of certain cases during the fw=1 fraction, trying to reduce the CEE impact. In practical terms, it may not always be possible to increase laboratory total flow rates: for instance, differential pressure limits, pump limits, fines migration (and other clay sensitivity issues), etc., may prohibit further increase.

DISCUSSION

The intercept method is a very interesting tool for determining relative permeability data, and was a good method to predict relative permeability under many conditions. However, it can fail when the capillary end effect (CEE) is not captured within the length of the core plug, i.e. the capillary regime extends beyond the injection face. This potential drawback was described in the original paper by Gupta and Maloney[1], and was the impetus to this review; since, in the experience of the authors, many commercial corefloods use short core plugs, with significant capillary artefacts observed in saturation profiles measured by *in situ* saturation monitoring (ISSM).

Failure to capture the CEE in the sample can derive from fractional flow rates that have not achieved steady state conditions (stable saturation and stable differential pressure). Laboratories should ensure that steady state is achieved by plotting production volumes and differential pressure as a function of time (most appropriately logarithm time or square-root time). Various scales should be employed for graphical axes when determining stability. Failure to capture CEE may also derive from inadequate viscous forces, i.e. Qt is too low and a laboratory should consider increasing Qt for that current and future fractional rates.

IM calculations are easy to implement, using graphical regression analysis as the functional process. Table 2 provides data results from standard Darcy calculations and IM calculations, from selected fractional rates of Case 3. The main functional regressions performed are:

- dP vs Qt
- Sw/(1-β) vs. β/(1-β)

Figure 1 shows examples of these functional regressions from three different fractional flow rates. The left plot shows an example where IM predicted kr, at low fw (0.1), with an excellent correlation. In Table 1 at this fraction (and other fractions that correctly predicted kr), a unique value of krw and kro can be observed for each Qt, except fw = 0.99 which exhibits a small error (± 0.0001mD = ± 0.25 %). The middle and right-hand plots show

examples when IM has failed to predict (fw = 0.999 & fw = 1). The tabular krw at these fractions are observed as non-unique values. For example, for fw = 0.999, the average krw is 0.0903 with a maximum error of 16.7%. However, it must be noted that average value is not the correct relative permeability (regression of just the higher Qt rates may improve the prediction). Observation of non-unique IM krw and/or kro can be used as a device to determine whether additional stabilisation time might be required or an additional, higher Qt may be required.

CONCLUSIONS

- The intercept method (IM) is a good prediction of relative permeability for a wide range of wetting states, relative permeability curves and capillary pressure, over a wide range saturation values. However, for certain systems, the validity of IM degrades at higher water saturations, most often in the krw curve.
- The successful application of IM is dependent on capturing the full capillary end effect within each flow rate at each fraction flow step.
- The validity of IM calculations at specific fractional flows is dependent upon each total flow rate achieving steady state conditions at that fractional rate step. This is particularly necessary at early and late fractions.
- It is easy for a laboratory to assess whether results correctly predict saturation and relative permeability at each fractional flow rate, i.e. results should be unique for each total flow rate at that fw. If not, the steady state criteria and/or total flow rates should be reviewed.
- In such circumstances, it may be necessary to increase total flow rate to achieve viable inputs for deriving correct values, however, laboratory limits and/or core sensitivities may preclude the practicality of this.
- Residual oil saturation cannot be guaranteed by performing these experiments. It thus remains, that residual oil saturation by purely flooding techniques may not be realised.
- It is strongly recommended to design the experiments using a flow simulator to assess what fractional flows and flow rate programming should be used to achieve reasonable results.

ACKNOWLEDGEMENTS

The authors would like to thank Dan Maloney and Robin Gupta for allowing us to use their original data and inputs, to begin our review of this interesting method.

REFERENCES

1. Gupta, R., Maloney, D., (2014), Intercept Method – A Novel Technique to Correct Steady-State Relative Permeability Data for Capillary End-Effect, *SPE Reservoir Evaluation & Engineering*, **SPE 171797**, doi:10.2118/171797-MS
2. Gupta, R., Maloney, D., (2015), "Applications of the Intercept Method to Correct Steady-State Relative Permeability for Capillary End-Effects", *International Symposium of the SCA*, **SCA2015-001**

3. Rapoport, L. A., and Leas, W. J., (1953) "Properties of Linear Waterfloods," *Society of Petroleum Engineers*, **SPE-213-G**, doi:10.2118/213-G.
4. Batycky, J.P., McCaffrey, F.G., Hodgins, P.K. and Fischer, D.B., "Interpreting Relative Permeability and Wettability from Unsteady State Displacement Measurements", Society of Petroleum Engineers, **SPE 9403**, doi: 10.2118/9403-PA
5. Chen, A. L, and Wood, A. C., (2001), "Rate Effects on Water-Oil Relative Permeability," *International Symposium of the SCA, Edinburgh*, **SCA2001-19**
6. van der Post, N., Masalmeh, S.K., Coenen, J.G.C., van der Gyp, K.H., and Maas, J.G., "Relative permeability, hysteresis and I-Sw measurements on a carbonate prospect", International Symposium of the SCA, Abu Dhabi, **SCA 2000-7**
7. Maas, J.G., Flemisch, B., Hebing, A., (2011), "Open Source Simulator DUMU^X Available for SCAL Data Interpretation", *International Symposium of the SCA*, **SCA2011-08**

Table 1: Summary of core properties, fluid properties, relative permeability and capillary pressure inputs

Case	Case 0	Case1	Case2	Case3	Case4	Case5
Core Properties						
Length [cm]	30.0	9.00	6.42	32.07	4.94	6.70
Diameter [cm]	3.81	3.81	3.75	3.704	3.80	3.74
Area [cm^2]	11.40	11.40	11.04	10.77	11.34	11.01
Bulk volume [cc]	342.03	102.61	70.84	345.50	56.03	73.69
Porosity [v/v]	0.250	0.215	0.231	0.333	0.245	0.277
Pore Volume [cc]	85.51	22.06	16.35	115.06	13.75	20.41
Reference permeability, k_{ref} [mD]	15	20	191	2800	2000	2.5
RQI [µm]		0.30	0.95	2.88	2.84	0.09
Corresponding Plug for Pc Data						
Klinkenberg permeability [mD]		13.88	175	2600	1700	2.7
Porosity [v/v]		0.204	0.236	0.315	0.214	0.204
RQI [µm]		0.26	0.86	2.85	2.80	0.11
Fluid Properties						
Water density [g/cc]	0.987	1	1.001	0.99	1.001	0.93
Water viscosity [cp]	0.332	1	0.901	0.58	1.301	0.38
Oil density [g/cc]	0.78	0.85	0.92	0.80	0.87	0.72
Oil viscosity [cp]	1.645	1.45	10.81	11.27	5.0	0.35
Relative permeability input – Corey model						
Swi [v/v]	0.100	0.250	0.131	0.150	0.077	0.122
Sor [v/v]	0.200	0.05	0.140	0.180	0.05	0.210
Krw'	0.65	0.40	0.40	0.25	0.75	0.62
Kro'	1.00	0.48	1.00	0.80	1.00	1.00
Nw	2	2.5	4.0	6.75	1.88	3.51
No	6	3.8	4.5	3.2	3.40	2.20
Capillary pressure input – Skjæveland model						
C_w	Tabular Input per SPE 171797	0.06	1.1	1.0	0.0	0.38
a_w		0.50	0.3	0.25	0.25	0.25
C_o		0.25	0.6	0.46	0.102	2.03
a_o		1.60	1.2	0.74	1.46	0.45
Total flow rates employed in the Intercept Model simulations						

Total flow rate 1 [cc/h]	30	30	30	30	30	5 (10)
Total flow rate 2 [cc/h]	60	60	60	60	60	10 (20)
Total flow rate 3 [cc/h]	120	90 (120)	90 (120)	90 (120)	90 (120)	20 (30)
Total flow rate 4 [cc/h]	240	120 (480)	120 (480)	120 (480)	120 (360)	30 (40)

NB. The bracketed total flow rates were those used at fw=1, in order to increase viscous forces and reduce the influence of capillary end effects.

Table 2: Case3 data table showing test parameters and Darcy analytical results

Total Q	fw	Avg Sw	dP	Darcy	
cc/h		v/v	psi	krw	kro
120	0.000	0.150	7.349	0.000	0.798
30	0.050	0.416	8.8	4.26E-04	0.158
60	0.050	0.414	17.370	4.33E-04	0.160
90	0.050	0.414	25.902	4.36E-04	0.161
120	0.050	0.413	34.435	4.37E-04	0.162
30	0.100	0.438	9.994	7.53E-04	0.132
60	0.100	0.437	19.719	7.63E-04	0.134
90	0.100	0.436	29.446	7.67E-04	0.134
120	0.100	0.436	39.172	7.68E-04	0.135
30	0.980	0.636	2.596	0.028	0.011
60	0.980	0.638	5.044	0.029	0.012
90	0.980	0.638	7.493	0.030	0.012
120	0.980	0.639	9.941	0.030	0.012
30	0.990	0.653	2.079	0.036	0.007
60	0.990	0.657	3.915	0.038	0.007
120	0.990	0.659	7.597	0.039	0.008
480	0.990	0.661	29.702	0.040	0.008
30	0.999	0.694	1.327	0.057	0.001
60	0.999	0.695	2.503	0.060	0.001
90	0.999	0.707	3.249	0.069	0.001
120	0.999	0.714	3.930	0.077	0.001
30	1.000	0.694	1.326	0.057	0.000
60	1.000	0.719	1.980	0.076	0.000
120	1.000	0.742	3.007	0.100	0.000
480	1.000	0.779	7.723	0.156	0.000

	ΔPI	Corr.DP	β	β/(1-β)	Sw/(1-β)	Sw_T	kew	keo	krw	kro
Swi	7.349	0.00				0.15		2235	0.00	0.80
	0.306	8.53	0.035	0.0359	0.431	0.412	1.235	457	4.41E-04	0.1633
fw1	0.306	17.06	0.018	0.0179	0.422	0.412	1.235	457	4.41E-04	0.1633
0.05	0.306	25.60	0.012	0.0120	0.419	0.412	1.235	457	4.41E-04	0.1633
	0.306	34.13	0.009	0.0090	0.417	0.412	1.235	457	4.41E-04	0.1633
	0.268	9.73	0.027	0.0275	0.450	0.435	2.166	380	7.74E-04	0.1357
fw2	0.268	19.45	0.014	0.0138	0.443	0.435	2.166	380	7.74E-04	0.1357
0.10	0.268	29.18	0.009	0.0092	0.440	0.435	2.166	380	7.74E-04	0.1357
	0.268	38.90	0.007	0.0069	0.439	0.435	2.166	380	7.74E-04	0.1357
	0.148	2.45	0.057	0.0603	0.674	0.640	84.32	33.5	0.0301	0.0120
fw7	0.148	4.90	0.029	0.0302	0.657	0.640	84.34	33.6	0.0301	0.0120
0.98	0.148	7.34	0.020	0.0201	0.651	0.640	84.33	33.5	0.0301	0.0120
	0.148	9.79	0.015	0.0151	0.648	0.640	84.33	33.5	0.0301	0.0120
	0.233	1.85	0.112	0.1264	0.736	0.662	113	22.3	0.0404	0.0079
fw8	0.233	3.68	0.060	0.0634	0.699	0.662	113.3	22.3	0.0405	0.0080
0.99	0.233	7.36	0.031	0.0317	0.680	0.662	113.3	22.3	0.0405	0.0080
	0.233	29.47	0.008	0.0079	0.666	0.662	113.2	22.3	0.0404	0.0080
	0.614	0.71	0.462	0.8603	1.292	0.715	295	5.76	0.1053	0.0021
fw9	0.614	1.89	0.245	0.3250	0.921	0.715	222.8	4.35	0.0796	0.0016
1.00	0.614	2.64	0.189	0.2329	0.871	0.715	239.6	4.68	0.0856	0.0017
	0.614	3.32	0.156	0.1851	0.847	0.715	253.9	4.95	0.0907	0.0018
	1.119	0.21	0.844	5.4015	4.445	0.784	1017	0	0.3634	0
fw10	1.119	0.86	0.565	1.2987	1.652	0.784	489.2	0	0.1747	0
1.00	1.119	1.89	0.372	0.5923	1.181	0.784	446.2	0	0.1594	0
	1.119	6.60	0.145	0.1694	0.911	0.784	510.5	0	0.1823	0

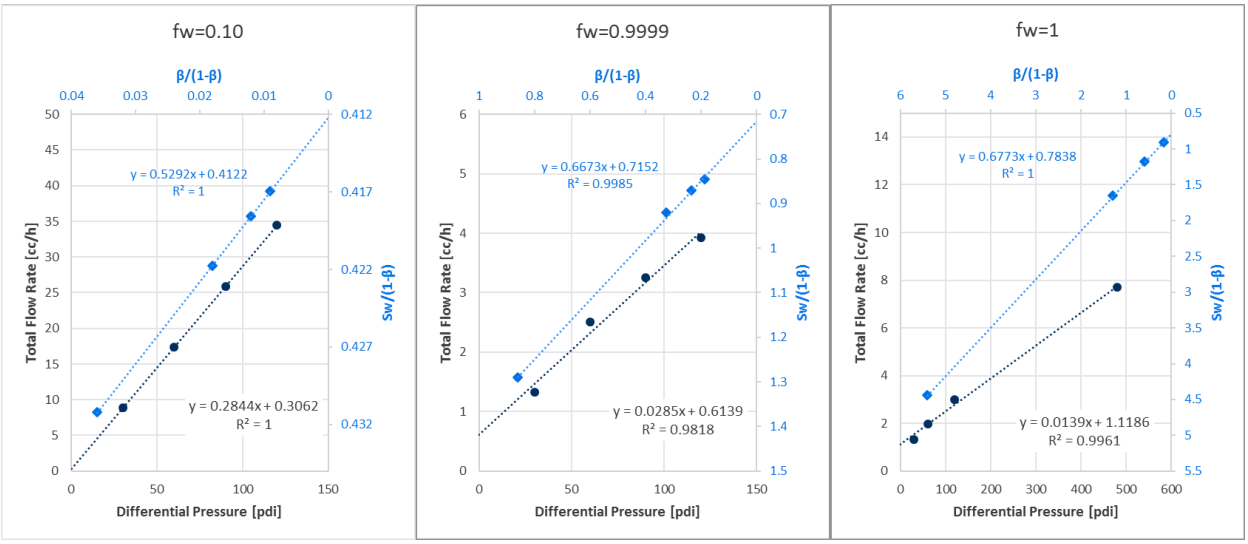

Figure 1: Case3 - example of Qt versus dP and Sw/(1-β) versus β/(1-β) at 4 total flow rates for 3 of the fractional flow rates (fw = 0.1, 0.9999 and 1), indicating the breakdown of the regression, particularly in dP at higher fw, hence breakdown of the intercept method

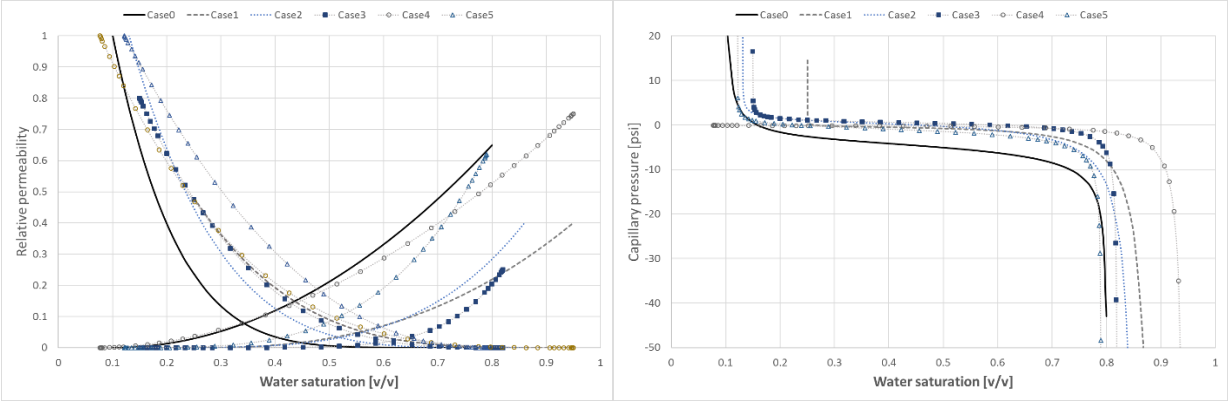

Figure 2: Summary of relative permeability and capillary pressure data for the case study samples, input to intercept method simulations

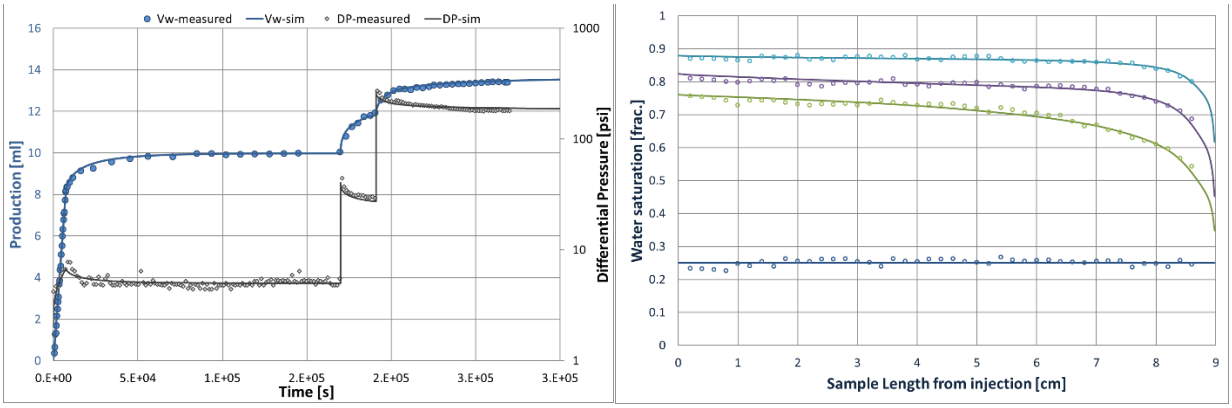

Figure 3: Case1 experimental data with simulated history match

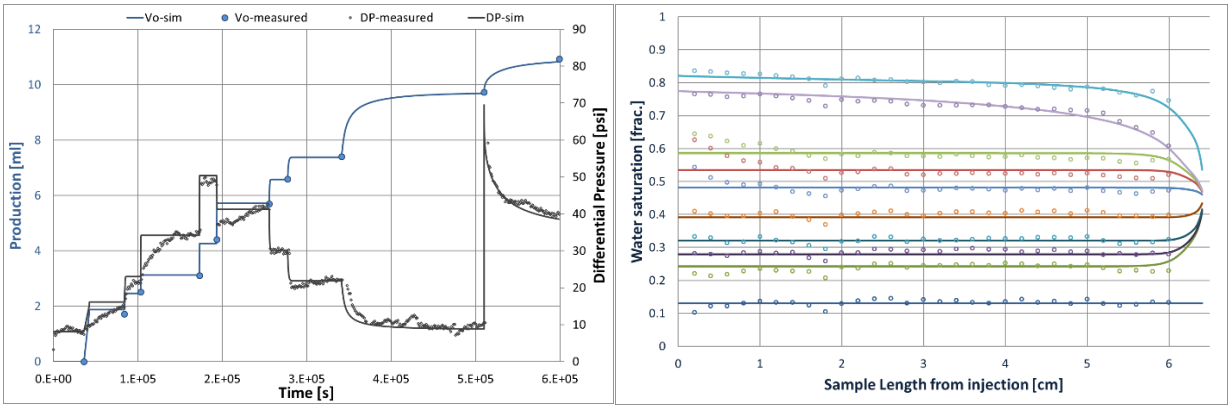

Figure 4: Case2 experimental data with simulated history match

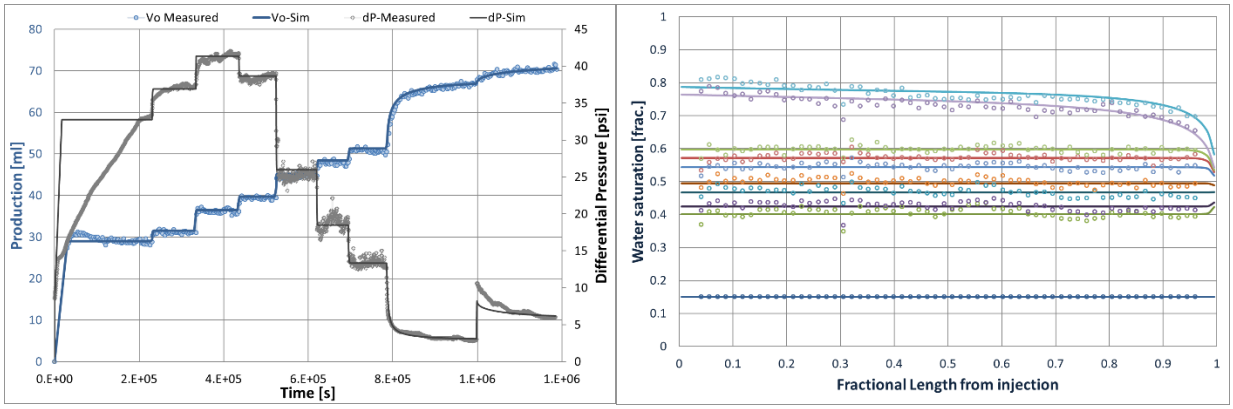

Figure 5: Case3 experimental data with simulated history match

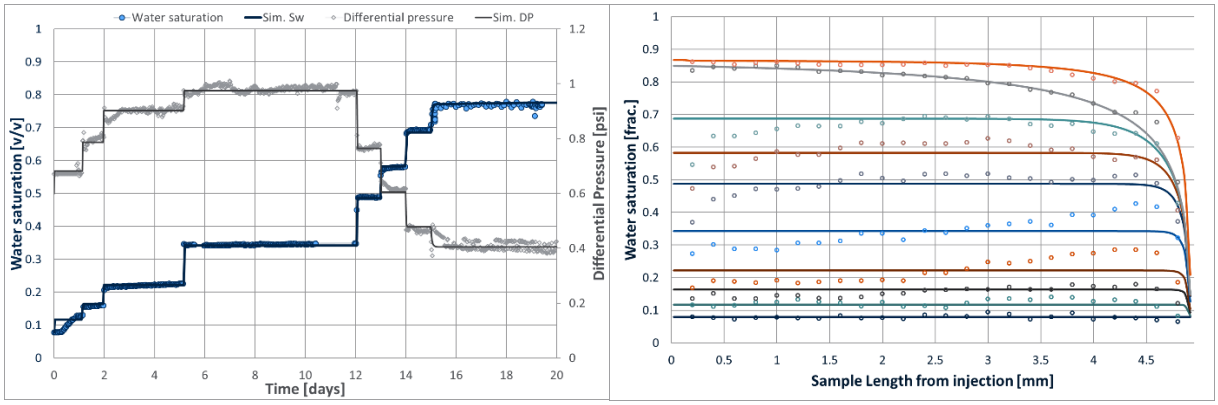

Figure 6: Case4 experimental data with simulated history match

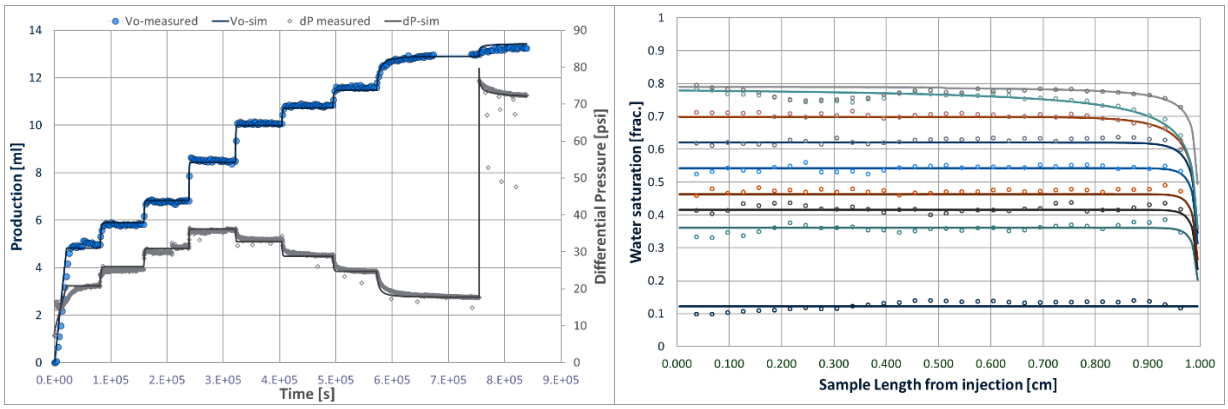

Figure 7: Case5 experimental data with simulated history match

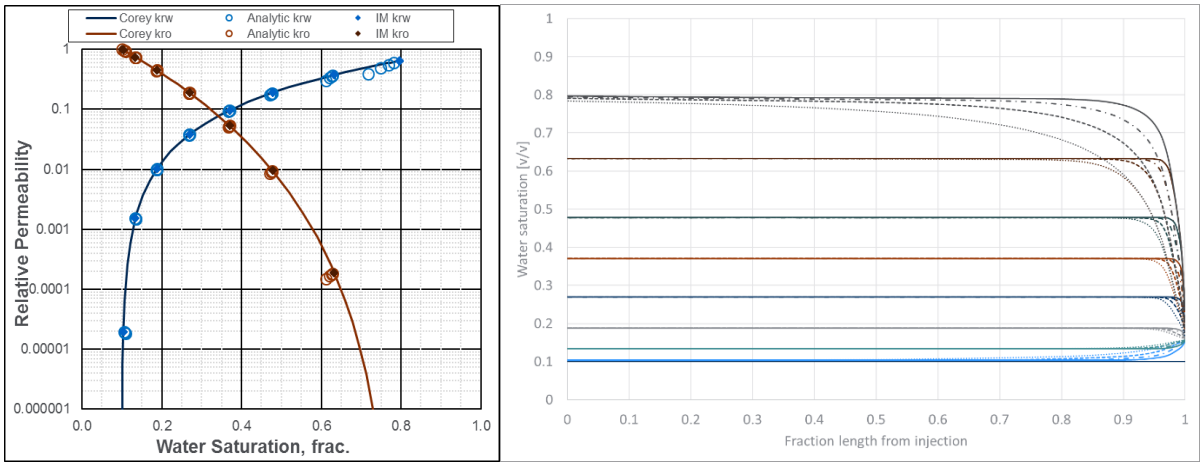

Figure 8: Case0 relative permeability curves (left), saturation profiles (right)

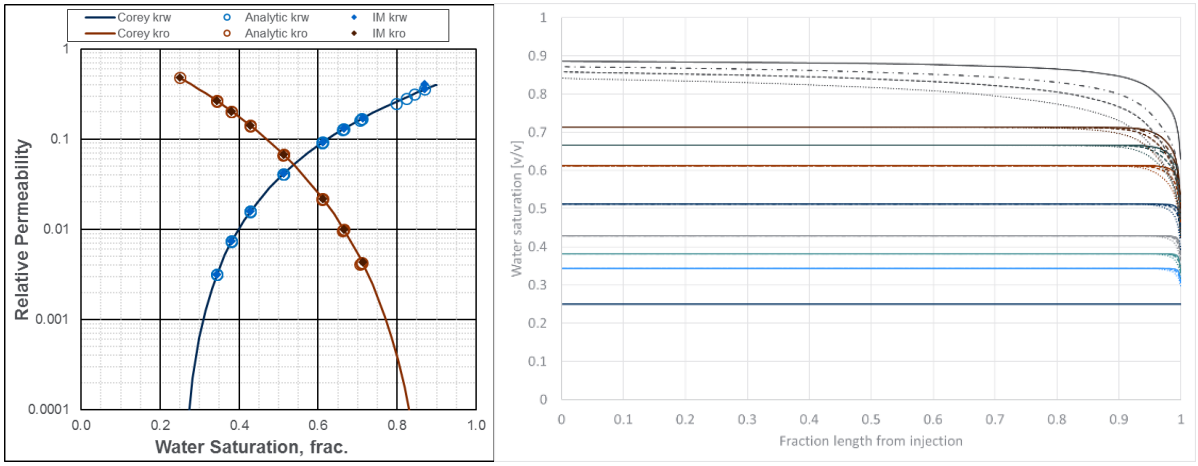

Figure 9: Case1 relative permeability curves (left), saturation profiles (right)

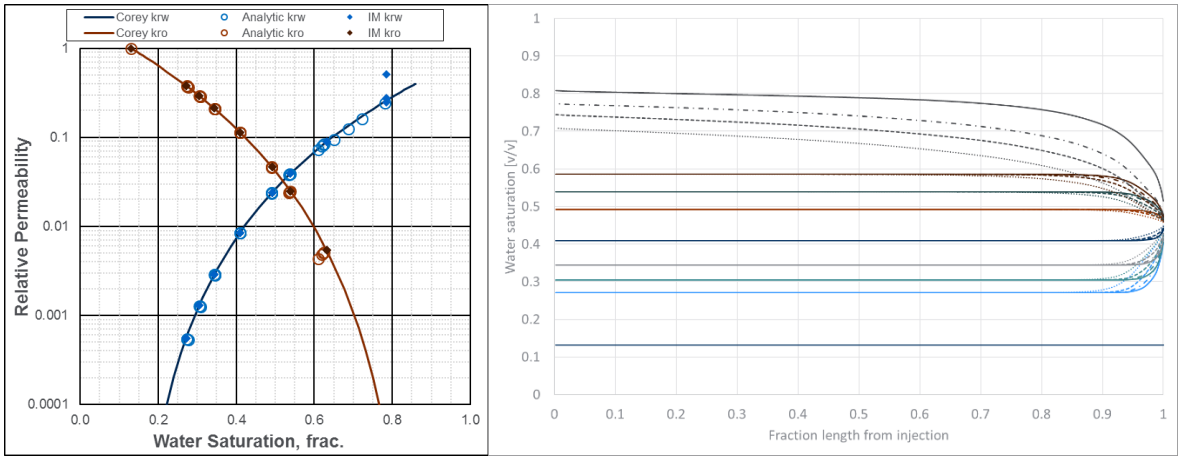

Figure 10: Case2 relative permeability curves (left) and saturation profiles (right)

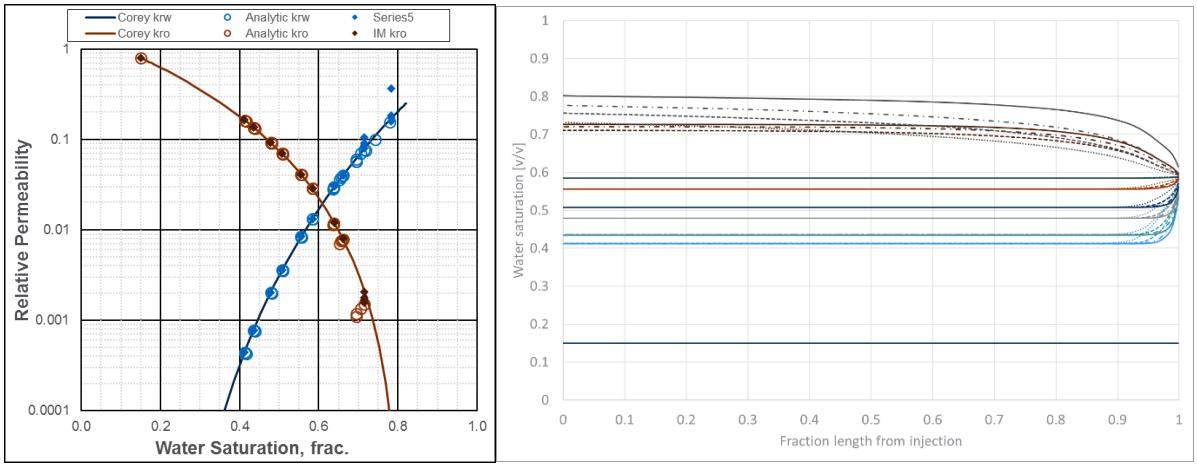

Figure 11: Case3 relative permeability curves (left) and saturation profiles (right)

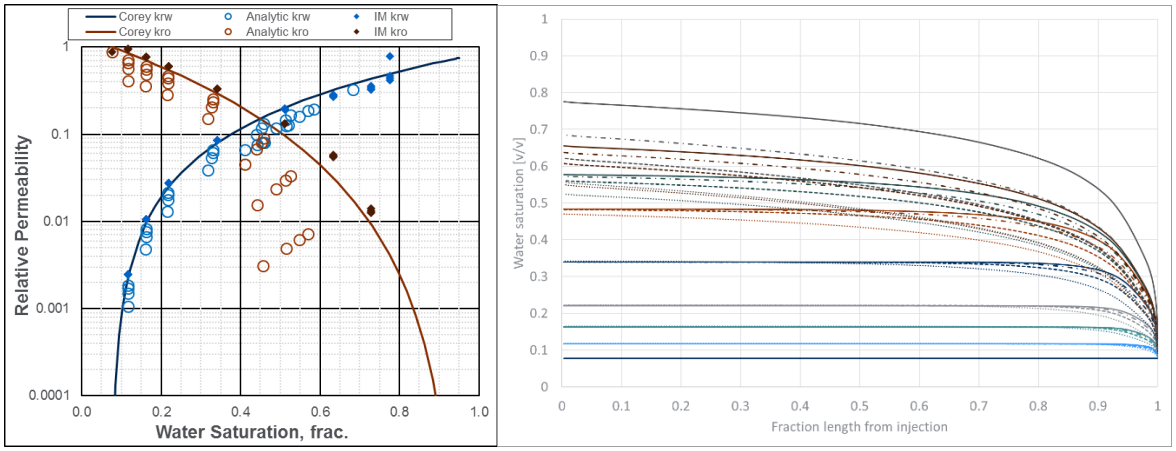

Figure 12: Case4 relative permeability curves (left) and saturation profiles (right)

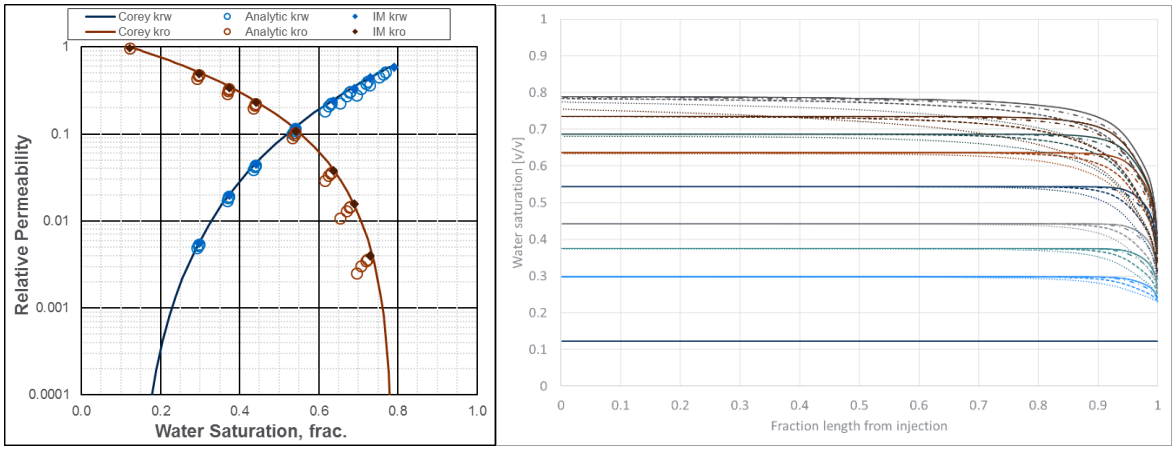

Figure 13: Case5 relative permeability curves (left) and saturation profiles (right)

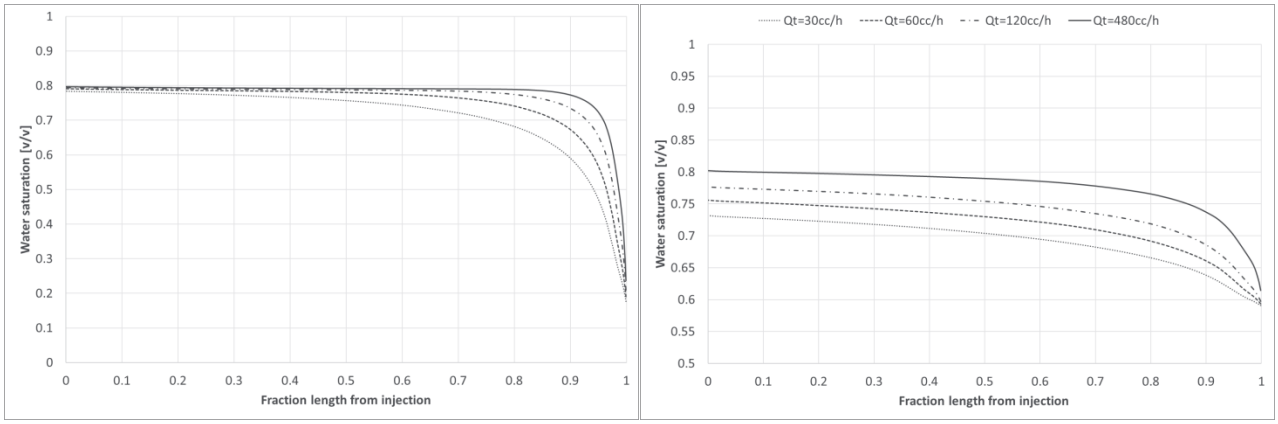

Figure 14: Case0 (left) and Case3 (right) saturation profiles for each total flow rate at fw=1, Case0 showing CEE effectively captured within the sample length (i.e. saturations resolving to a unique value at the injection face), Case3 showing unresolved saturation profiles.

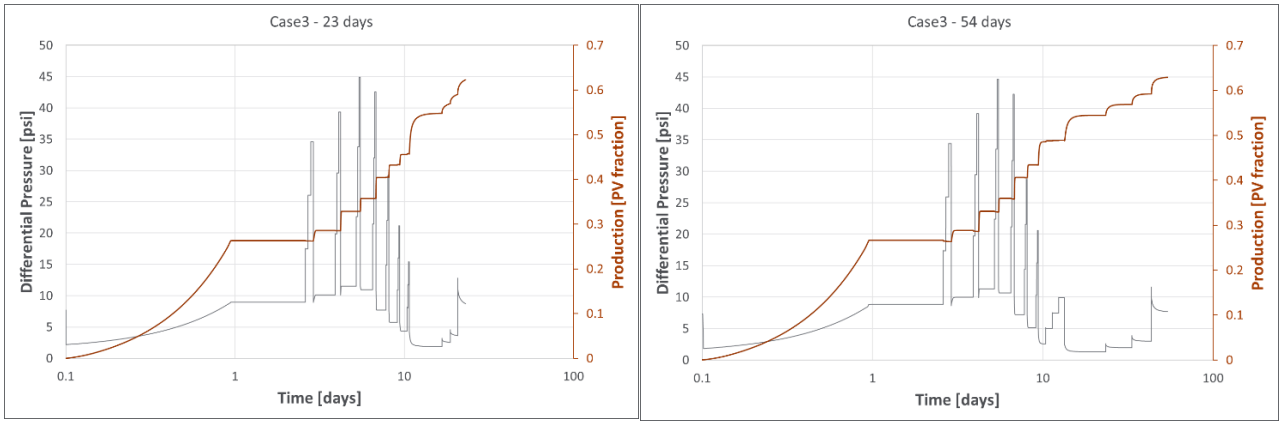

Figure 15: Example of production data (Case3) using different run times to attempt to achieve steady state conditions, thus optimise the IM results. The final 3 rates in the shorter run (left) have not achieved steady state, additional time was used for the next simulation (right). However, note the final rate in the longer run (right – 44-54 days) yet may not have achieved steady state.